An oxidation-sensitive dextran-based polymer with improved processability through stable boronic ester groups

Amanda J. Manaster[1], Cole Batty[2], Pamela Tiet[2], Annabelle Ooi[1], Eric M. Bachelder[2], Kristy M. Ainslie[2], Kyle E. Broaders[1]

[1]Department of Chemistry, Mount Holyoke College, South Hadley, Massachusetts 01075, USA

[2]Eshelman School of Pharmacy, Division of Pharmacoengineering and Molecular Pharmaceutics, The University of North Carolina at Chapel Hill, Chapel Hill, North Carolina 27599, USA

KEYWORDS oxidation, degradable polymers, boronic esters, dextran, immunotherapy, microparticles.

ABSTRACT

Particulate immunotherapy holds promise to vaccinate or treat a broad array of illnesses, including cancer, infectious diseases, and autoimmune disorders. The rate of antigen release from nano/microparticles (MPs) can impact both the type and quality of the immune response they elicit. The lysosomes of antigen presenting cells are highly oxidizing. Thus, an oxidation-sensitive vehicle could enable a significant advancement in effective MP immunotherapy. One promising class of materials being developed toward this end are aryl boronate-modified dextran polymers. The boronic esters used for oxidation-sensitive materials and sensors are typically made using pinacol (Pin) as a diol. However, Pin-based aryl boronate-modified polymers are capable of transesterifying with biogenic diols, which can lead to undesirable interactions and poor material properties. To solve this, pinanediol (PD) was used in place of Pin in the synthesis of an aryl-boronate modified dextran polymer (PDB-Dex), yielding a highly stable boronic ester. This modified dextran reverses its water solubility as desired, and improves on Pin-based materials by maintaining its solubility in organic solvents. MPs could be prepared by emulsion, nanoprecipitation, and electrospray techniques. Hydrogen peroxide-triggered degradation of microparticles was quantified colorimetrically, and the mechanism was probed using ^{1}H-NMR. Preliminary in vitro studies show low cytotoxicity and the ability to deliver an immunostimulatory agent.

Introduction

Particulate carriers hold the potential to boost the flexibility, feasibility, and efficiency of immunotherapy.[1,2] They can encapsulate proteins and small molecules alike through physical entrapment, and can enable a wider range of immune responses than traditional formulations, such as cytotoxic T-cell responses needed for cancer vaccines.[1] Additionally, synthetic nano/microparticles (MPs) can potentially mitigate vaccine toxicity.[3] Similar to traditional immunotherapy, the most common targeting modality for MPs is based on the route of administration. After intramuscular or subcutaneous injection, components are passively taken up by antigen presenting cells (APCs) like dendritic cells (DCs) and macrophages. Moreover, MPs can passively target APCs because phagocytic cells are capable of engulfing material larger than 200 nm, while non-phagocytic cells are unable to phagocytose MPs of this size.[2-6] The route of antigen processing within APCs can drastically influence the type and strength of the resulting response.[7] Controlling the rate of cargo release and the conditions for release can affect antigen processing within APCs, and therefore influence vaccine efficacy, and the relative contribution of cellular and humoral immune responses.[4-5]

Using oxidation as a trigger for cargo release is especially appealing. Aerobic metabolism entails the reduction of oxygen, a process that inherently generates reactive oxygen species (ROS). These species are normally balanced by cellular antioxidants to maintain oxidative equilibrium; the buildup of these species can cause degradation of nucleic acids, proteins, and lipids in a process collectively termed oxidative stress.[8] Although often destructive, the ability to direct oxidative stress is among the oldest and most effective forms of immune response against infectious agents. In mammals, for example, neutrophils attack invading microorganisms by generating and releasing a variety of ROS in a process called oxidative burst. Oxidation also plays an important role in the

destructive action of lysosomes within APCs. These cells digest and prepare antigen-derived peptides for activation of the adaptive immune system, and are thus the targets for vaccines and other immunotherapies.

Oxidation sensitivity has been used as a means for triggering release from a variety of polymeric materials[9]. Crosslinked poly(propylene sulfide) has been used in the design of nanoparticles that execute the release of hydrophobic drugs upon oxidation to poly(sulfone).[10] This transition from sulfide to sulfone leads to a large change in hydrophobicity, which induces particle swelling and cargo release. A similar strategy of solubility modulation by oxidation has been achieved using selenium.[11] Additionally, inorganic carriers can release surface-bound small molecules upon oxidation by conversion of stable Si–Si bonds to hydrolytically labile Si–O bonds.[12] Although each of these methods have their own benefits and drawbacks, the functional group most commonly used to confer oxidation sensitivity to a polymeric material is a boronic ester.

Boronic ester-containing materials have been used in diverse settings to form delivery vehicles, cell capture materials, chromatographic media, and molecular sensors.[13] A large portion of these materials feature arylboronic esters to confer biologically accessible oxidation sensitivity.[9,14] These arylboronic esters can be oxidized under physiological conditions and yield phenols, which can be designed to undergo further self-immolative reactions. Despite their growing ubiquity, boronic esters are nearly always made using a single diol: pinacol (Pin). The identity of this ester group, however, can have important consequences for the properties and behaviors of arylboronic esters, especially in the context of polymeric materials.

In previous work, pinacol arylboronic esters were used to confer oxidation-sensitive solubility switching to dextran.[15] This material, originally termed Oxi-Dex and hereafter referred to as PinB-Dex, is water-insoluble until degradation initiated by hydrogen peroxide, whereupon the major

degradation byproduct is dextran, a polymer that is Generally Recognized As Safe (GRAS) by the FDA and often used in the production of materials for drug delivery.[16] Although PinB-Dex possesses the desired oxidation sensitivity, its solubility in organic solvents diminishes upon concentration, making material processing both difficult and problematic to reproduce. These problems could be somewhat ameliorated through treatment with hot methanol, but could not be satisfactorily solved. The loss of organic solubility of PinB-Dex is hypothesized to arise from boronic ester transesterification causing inter-strand crosslinks between boronic groups on one strand and diols present on adjacent strands (Scheme 1). The transesterification reaction between boronic esters and diols is strongly influenced by pH, and by the identity of the ester diol and the diol that supplants it.[17]

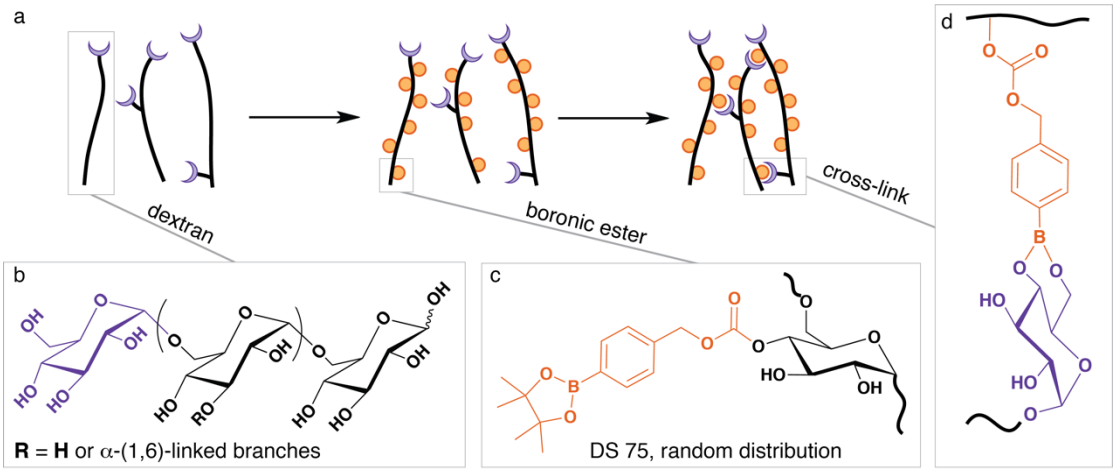

Scheme 1. Proposed mechanism of PinB-Dex crosslinking. a. After modification of dextran with boronic ester groups (orange circles), non-reducing ends (purple crescents) generate interstrand links. **b.** Structure of dextran highlighting ~5% α-(1,3) branching. c. Structure of PinB modifications. d. Proposed linkage between polysaccharide non-reducing ends and boronic esters.

Although the ability of arylboronic esters to transesterify has been well-characterized, less is known about the effect of boronic ester identity in the context of oxidation sensitive materials. We

hypothesized that undesired cross-linking was the cause of the poor material properties observed in PinB-Dex, and that inhibiting this reaction might yield more tractable material. To test this hypotheses, we altered the boronic ester by employing pinanediol (PD) in place of Pin, as PD is known to form extremely kinetically and thermodynamically stable boronic esters.[18] We further hypothesized that this change would only minimally impact the oxidation of the boronic ester because of the small size of hydrogen peroxide.

Here we report on the synthesis, and characterization of PDB-Dex, a dextran modified with a carbonate-linked arylboronic ester of PD. After formation into MPs, its suitability for use in delivery applications was assessed in cell-based proof of concept delivery experiments.

Materials and Methods

General methods and equipment:

Unless otherwise specified all reagents were purchased from Sigma Aldrich, Acros Organics or Oakwood Chemical and used without further purification without otherwise specified. Water (dd-H_2O) for buffers and particle washing steps was purified to a resistance of 18.2 MΩ using a Milli-Q Advance a10 purification system (Millipore, USA). H^1 spectra were recorded at 400 MHz and C^{13} spectra were recorded at 100 MHz on a Bruker AVANCE 400 with BBI broadband probe and variable temperature unit. Infrared spectra were collected using a Bruker Alpha with ATR. A SFX550 Ultrasonicator (Branson Ultrasonics, USA) was used for particle preparation via single emulsion. Lyophilization was done on a FreeZone 4.5 (Labconco, USA). Dynamic Light Scattering and Zeta Potential measurements were made using a Zetasizer Nano ZS (Malvern Instruments, UK). THF and DCM were stored and dispensed from a PureSolv solvent purification system (Inert, USA). Large scale centrifugations (more than 1.5 mL) were done in a Sorvall

Legend X1 with a fixed angle rotor (ThermoFisher Scientific, USA). Small scale centrifugations were done with a MiniSpin (Eppendorf, Germany).

Synthesis of Pinacol boronic ester (PinB Ester) and Pinanediol boronic ester (PDB Ester)

Pinacol (2.91 g, 24.6 mmol) was combined with phenylboronic acid (1.00 g, 8.20 mmol) in tetrahydrofuran (10 mL). The reaction was mixed on a rotisserie overnight and dried over sodium sulfate. The solution was concentrated under vacuum and dissolved in ethyl acetate (20-40 mL) and washed with water (3 x 10 mL) and brine (10 mL). The same procedure was repeated with the replacement of pinacol with pinanediol (1.40 g, 8.20 mmol). Spectral data matched literature values.[19,20] For NMR, PinB Ester and PDB Ester were dissolved in deuterated dimethyl sulfoxide and standard proton NMR spectra were collected. Spectra for pure pinanediol and pinacol were also collected for a baseline. Subsequently, PinB ester and PDB Ester were combined with dextran (50 mg/mL) in d-DMSO and time-lapse spectra were collected for 12 and 36 hours.

Synthesis of boronic ester 1

Pinanediol (4.83 g, 28.37 mmol) was combined with 4(hydroxymethyl)phenyl boronic acid (4.31 g, 28.37 mmol) in tetrahydrofuran (43.2 mL). Sodium sulfate (7 g) was added to the reaction and stirred overnight. The solution was filtered and concentrated under vacuum. Dry column vacuum chromatography was used to purify the product (0 – 80% EtOAc in Hex, Rf 0.39 in 25% EtOAc in Hex). Fractions were combined and concentrated *in vacuo* to a pale yellow oil (7.6 g, 95% yield). 1H NMR (400 MHz, $CDCl_3$-d) δ 7.84 (d, J = 8.1 Hz, 2H), 7.40 (d, J = 8.2 Hz, 2H), 4.75 (d, J = 5.6 Hz, 2H), 4.48 (dd, J = 8.8, 1.9 Hz, 1H), 2.47 – 2.41 (m, 1H), 2.29 – 2.14 (m, 2H), 2.07 (s, 1H), 1.97 (s, 1H), 1.77 (d, J = 11.9 Hz, 1H), 1.34 (s, 3H), 1.28 (t, J = 7.1 Hz, 1H), 1.23 (d, J = 10.9 Hz, 1H), 0.92 (s, 3H). 13C NMR (101 MHz, Chloroform-d) δ 143.94, 135.09, 126.14, 86.31, 78.27, 65.27, 60.44, 51.42, 39.54, 38.21, 35.57, 28.72, 27.12, 26.50, 24.07, 21.08, 14.22.

Synthesis of CDI-activated ester 2

Pinane boronate **1** (7.6 g, 26.56 mmol) was dissolved in DCM (150 mL) in a dry flask under Ar, and then CDI (8.61 g, 53.11 mmol) was slowly added. After 30 minutes, the reaction was concentrated *in vacuo*, and redissolved in EtOAc (75 mL). This solution was washed with water (3 x 10 mL), 5% $KHSO_4$ (3 x 10 mL), and brine (2 x 10 mL). The organics were then dried over $MgSO_4$ and concentrated *in vacuo* to a thick, yellow oil (8.63 g, 86% yield). 1H NMR (400 MHz, $CDCl_3$-d) δ 8.17 (t, J = 1.1 Hz, 1H), 7.89 (d, J = 8.1 Hz, 1H), 7.50 – 7.42 (m, 2H), 7.08 (dd, J = 1.7, 0.8 Hz, 1H), 5.45 (s, 1H), 4.49 (dd, J = 8.8, 1.8 Hz, 1H), 2.51 – 2.38 (m, 1H), 2.31 – 2.14 (m, 1H), 2.04 – 1.93 (m, 1H), 1.73 (s, 1H), 1.51 (s, 2H), 1.34 (s, 2H), 1.32 – 1.17 (m, 1H), 0.91 (s, 2H). 13C NMR (101 MHz, Chloroform-d) δ 148.59, 137.16, 136.71, 135.31, 130.71, 127.81, 117.16, 86.49, 78.38, 69.73, 60.40, 51.38, 39.51, 38.22, 35.53, 28.70, 27.10, 26.49, 24.06, 21.07, 14.22, 1.04.

Synthesis of PDB-Dex

In a dry flask under argon, dextran from *Leuconostoc mesenteroides* (9-11 KDa, Sigma-Aldrich, 1.90 g, 11.70 mmol) was dissolved in DMSO (20 mL). **2** (8.90 g, 23.41 mmol) was added, and, after complete dissolution, DMAP (3.15 g, 25.75 mmol) was added. Solution was kept under Argon overnight. The solution was precipitated into 5% $KHSO_4$ (~ 50 mL) and centrifuged (12,000 x g, 10 min) into a pellet. The supernatant was discarded and the resulting pellet was washed by resuspending in 5% $KHSO_4$ (40 mL), and centrifuging again. The pellet was then washed again with $KHSO_4$ (40 mL) and once with ddH_2O (30mL). After discarding the supernatant, the pellet was frozen using liquid nitrogen and lyophilized. White solid was then redissolved in EtOAc (30 mL) and extracted with 5% $KHSO_4$ (3 x 10 mL), H_2O (2 x 10 mL), and brine (2 x 10 mL). The

organic phase was dried over $MgSO_4$, filtered, and then precipitated dropwise into hexanes (100 mL), pelleted via centrifugation and concentrated *in vacuo* to yield a white solid (4.8 g, 83% yield).

Characterization of degradation byproducts and kinetics by NMR

To determine the byproducts, PDB-Dex was dissolved in deuterated PBS (0.2mg/mL) and combined with 50 mM Na_2O_2. For kinetics, PDB-Dex was dissolved in deuterated PBS (0.1 mg/mL) and combined with 1 mM Na_2O_2. A standard proton NMR was run for 60 hrs and 64 scans were taken every 10 minutes.

Preparation of Emulsion Microparticles

Sub-micron Single Emulsion Particles were prepared according to a procedure adapted from Beaudette et al.[21] Briefly, PDB-Dex (100 mg) was dissolved in dichloromethane (2 mL). This solution was added to an aqueous solution of poly(vinyl alcohol) (PVA, MW = 13,000 -23,000 g/mol, 87-89% hydrolyzed) (6 mL, 1% w/w in PBS) and emulsified by sonicating for 45 s on ice using a probe ultrasonicator (with the following settings: 45 s total sonication cycling between 0.8 s on and 0.2 s off with power at 35% and using a 1/2- inch flat tip. The resulting emulsion was poured into a second PVA solution (100 ml, 0.3% w/w in PBS) and stirred for 5.5 h allowing the organic solvent to evaporate. The particles were isolated by centrifugation (14,000 x g, 5 min) and washed with dd-H2O by vortexing and sonication followed by centrifugation and removal of the supernatant. The washed particles were resuspended in dd-H2O and lyophilized to yield a white fluffy solid (60mg, 60% yield). For dynamic light scattering, PDB-Dex was suspended in PBS (0.1 mg/mL), briefly sonicated and transferred to a standard disposable polystyrene cuvette. Measurements were taken at 37˚C using a Zetasizer Nano ZS (Malvern, UK).

Preparation of Nanoprecipitation Microparticles

Nanoprecipitations were prepared according to a procedure adapted from Liebert et al.[22] PDB-Dex or PinB-Dex were dissolved in acetone (100 μL, 4 mg/mL) then added to ddH_2O (2 mL). MP suspensions were analyzed without further purification.

Scanning electron microscopy

Emulsion MPs were characterized by scanning electron microscopy using a Quanta 200 SEM (FEI, USA). Particles were suspended in dd-H_2O at a concentration of 1 mg/mL and the resulting dispersions were dripped onto silicon wafers. After 15 min, the remaining water was wicked away using the corner of a KimWipe and the samples were allowed to air dry. The particles were then sputter coated with ~5 nm of a palladium/gold alloy and imaged at 5.0 kV in Secondary Electrons mode. Electrospray MPs were characterized as follows: PDB-Dex and resiquimod loaded PDB Dex MPs were electrosprayed directly onto the surface of an aluminum pin (Ted Pella, Inc., Redding, CA). SEM images were acquired using an S-4700 scanning electron microscope (Hitachi High Technologies, Schaumburg, IL). ImageJ software was used to analyze MP diameter with n > 30 MPs analyzed per sample.

Bulk Degradation of Emulsion Microparticles

PDB-Dex emulsion MPs were suspended at a concentration of 5 mg/mL in 1 mL solutions of PBS containing 0 mM, 0.05 mM, 0.1 mM, or 1.0 mM H_2O_2 in triplicate. These samples were placed on an Eppendorf Thermomixer-R (Fisher Scientific, USA) heating block with shaking at 37˚C. Aliquots (75 μL) were taken over the course of the following 70 hours, centrifuged at 10,000 x g for 30 s and the supernatant was stored at 4˚C. A Micro Bicinchoninic Assay (BCA, Thermo Scientific, USA) was performed to measure the release of dextran from degrading MPs according to literature with slight alterations.[23] Briefly, in a clear polystyrene 96-well plate, supernatants of aliquots taken from degrading microparticle suspensions (above, 50 μL) were mixed with KI

(1%(w/v), 20 μL) to catalytically decompose residual H_2O_2. After 3 h, working reagent was prepared according to manufacturer protocol and added to each well (200 μL). The plate was then incubated at 37°C for 3 hours and absorbance was measured at 562 nm on a SpectraMax M5e Multimode Plate Reader (Molecular Devices, USA).

Electrosprayed PDB-Dex MPs

PDB-Dex was further purified for electrospray by dissolution in THF and centrifugation at (22,000 x g, 1 h)**.** The supernatant was transferred into a scintillation vial and concentrated on a rotary evaporator, then lyophilized to remove all residual water and THF. Resiquimod-loaded PDB-Dex MPs were fabricated using an electrohydrodynamic spraying (ES) method similar to that previously reported.[24] A stainless steel plate was exposed to UV light for 1 h and heat treated at 265° C for 1 h to sterilize and reduce any endotoxin. PDB-Dex and resiquimod were dissolved in a 95:5 ethyl acetate:n-butanol mixture (1% total wt. solids) . A syringe pump was used to pump the resulting solution through an 18G needle mounted over the steel plate with a flow rate of 0.2 mL/h. The needle and steel plate were charged at -5 kV and +2.5 kV, respectively, using high voltage power sources (Gamma High Voltage Research Inc., Ormond Beach, FL). MPs were collected on the plate for 12.5 h. PDB-Dex blank MPs were fabricated by the same process without resiquimod in the sprayed solution.

Resiquimod quantification

Resiquimod-loaded PDB-Dex MP loading was quantified by measuring fluorescence.[24] Samples were prepared in triplicate and dissolved in DMSO. These were loaded onto a solvent resistant 96-well plate and quantified using a standard curve generated from free resiquimod in DMSO based on fluorescence (excitation: 260 nm, emission 360 nm) using a SpectraMax M2 microplate reader (Molecular Devices, USA). Blank PDB-Dex MPs were used to measure the background signal

which was subtracted from MP-containing wells. Encapsulation efficiency of Resiquimod in PDB-DEX MPs was calculated as shown:

$$Encapsulation\ efficiency(\%) = \frac{Experimental\ resiquimod\ loading}{Theoretical\ resiquimod\ loading} \times 100$$

Resiquimod release profile

Resiquimod loaded and blank MPs were suspended in microcentrifuge tubes (50 μg/mL, PBS pH 7.4) with or without H_2O_2. The suspensions were incubated at 37 °C on a shaking heating block. At specified timepoints, 100 μL of each suspension was removed and supernatant was isolated by centrifugation, and stored in a 96 well plate at −20 °C. Endpoints were collected by complete degradation of a final aliquot. Fluorescence was measured after all timepoints were collected using a microplate reader. The fluorescence of blank MPs was subtracted as background, and the intensities were normalized to the endpoint measurement.

***In vitro* cell viability analysis**

Balb/c mouse (Jackson Laboratory, Bar Harbor ME) bone marrow derived dendritic cells (BMDCs) were prepared and cultured using a previously published protocol.[25] Metabolic activity (viability and proliferation) of BMDCs was analyzed using a 3-(4,5-dimethylthiazol-2-yl)-2,5-diphenyltetrazolium bromide (MTT) assay after treatment with resiquimod or resiquimod-loaded PDB-Dex MPs at concentrations ranging from 0 to 250 ng resiquimod/mL. Cells were seeded in 200 μL of media overnight in a 96-well plate at 25,000 cells/well before incubation. They were then treated with different experimental groups for 72 h. Cells treated with blank PDB-Dex MPs, DMSO at maximum concentration, media only, or lipopolysaccharide (LPS, 100 ng/mL) were included as controls. The supernatant was removed and retained for future use. MTT solution (0.5 mg/mL) was added to each well (150 μL), including 3 blank wells (media only). The plate was incubated at 37°C for 1 h. Media was removed from each well, and formazan crystals were

dissolved in 100 μL of isopropanol. The absorbance of the resultant solution was measured at 560 nm using a SpectraMax M2 microplate reader. The background absorbance at 670 nm was also measured and subtracted from every well. Blank wells (media only) also served as background.

Cytokine quantification

BMDCs were prepared and cultured with the same method cited above. Secretion of IL-6 and TNF-α from BMDCs was analyzed by enzyme-linked immunosorbent assay (ELISA) after treatment with resiquimod or resiquimod-loaded PDB-Dex MPs at doses ranging from 0 to 250 ng/mL. Cells were seeded in 200 μL of media overnight in a 96-well plate at 25,000 cells per well before incubation with different treatment groups for 24 or 72 h. Cells treated with equivalent masses of blank PDB-Dex MPs, media only, or lipopolysaccharide (LPS, 100 ng/mL) were included as controls. The supernatants from the 24 and 72 h conditions were collected and analyzed for IL-6 and TNF-α according to the manufacturer's instructions (Fisher Scientific, Hampton, NH).

Results and Discussion

To test the hypothesis that significant transesterification of boronic esters may be occurring in PinB-Dex, we performed a simple displacement experiment (Figure 1a). Phenylboronic Pin ester (PinB-Ester) was combined with dextran in DMSO-d6, and the reaction was monitored *in situ* through NMR spectroscopy. Within 12 h, appearance of free Pin and concomitant reduction of ester were observed. Importantly, no change was observed in the absence of dextran. Although the boronic esters formed with the cis-1,2 diols along the dextran backbone are expected to be relatively unstable,[26] the branch and chain ends possess 1,3 diols, which can form more stable dioxaborinanes. Based on anomeric peak integration in D_2O, the dextran used had 2.9% branching

(Figure S1),[27] and an additional 1.6% of anhydroglucose residues (AGUs) are chain termini. Thus 4.5% of AGUs are expected to be able to form stable boronic esters. Based on these estimates, approximately 39% of available 1,3 diols participated in transesterification. The appearance of free pinacol in this experiment confirms that transesterification can occur between dextran and pinacol boronic esters, and supports the model wherein 1,3 diols are the most significant contributors to this phenomenon. Importantly, this transesterification occurs in solution; in precipitated polymers, the high local concentration may accelerate the reaction significantly.

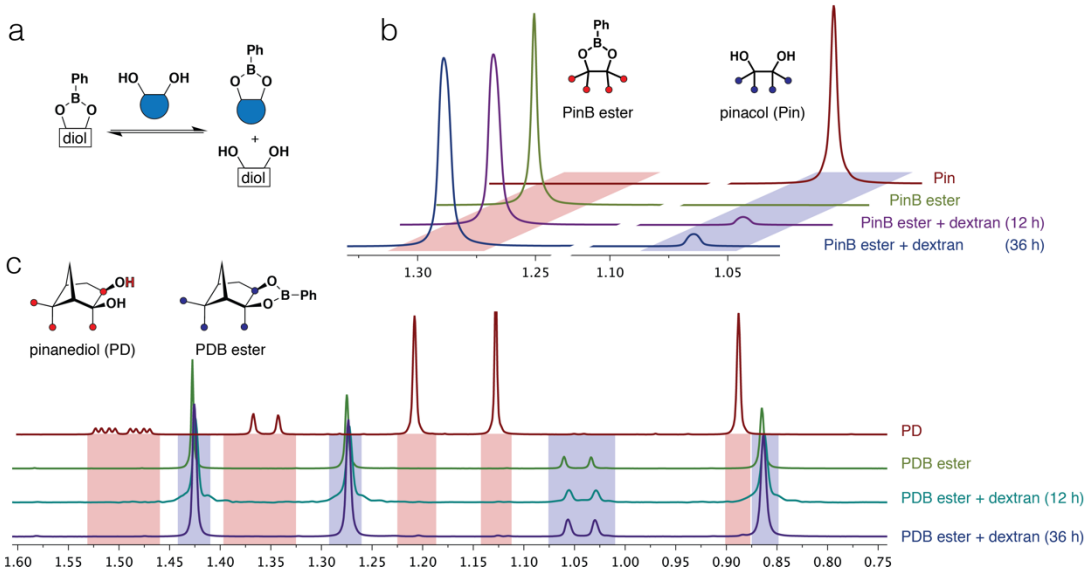

Figure 1. Comparative binding of pinacol vs pinanediol esters and dextran measured by H1-NMR. a) Boronic esters were combined with dextran and the release of free diol was observed. b) Free pinacol appears in solution within 12 h indicating transesterification with dextran. c) No PD is liberated from PDB-Ester in this time.

Having developed a proxy to measure the crosslinking propensity of PinB-Dex, we sought to develop a system that would resist crosslinking. Boronic esters have been found to be most thermodynamically stable when formed with diols featuring rigid coplanar cis-1,2 diols.[28]

Additionally, because transesterification occurs through an associative process, steric bulk has been observed to significantly slow the kinetics of transesterification. Among the most kinetically and thermodynamically stable boronic esters in the literature is that formed with PD.[18,28] To test whether replacement of Pin with PD in boronic esters might block crosslinking, we prepared phenylboronic acid PD ester (**PDB Ester**), and tested the ability for dextran to displace PD (Figure 1b). In contrast to **1**, **2** is completely unaffected by the presence of dextran, even after 36 h. This indicates that PDB ester is significantly more stable, slow to exchange, or both, than PinB ester.

Based on this lead, we set out to synthesize PDB-Dex (Scheme 2). 4-(hydroxymethyl)phenylboronic acid was esterified with PD, and then activated using carbonyldiimidazole (CDI). DMAP-catalyzed addition to dextran yielded a water-insoluble material that could be redissolved freely in common organic solvents including ethyl acetate and dichloromethane. This solubility was retained through several rounds of concentration and redissolution and did not diminish over a period of weeks. Although PDB-Dex is insoluble in water, it dissolves readily upon addition of hydrogen peroxide, indicating that PD does not block boronic ester oxidation. This degradability aided analysis as well: although the ^{1}H NMR of PDB-Dex proved difficult to interpret, analysis of its degradation products provided insight into the composition of PDB-Dex. An average of 0.75 modifications per AGU were found, corresponding to an overall Mn of 22-27 KDa.

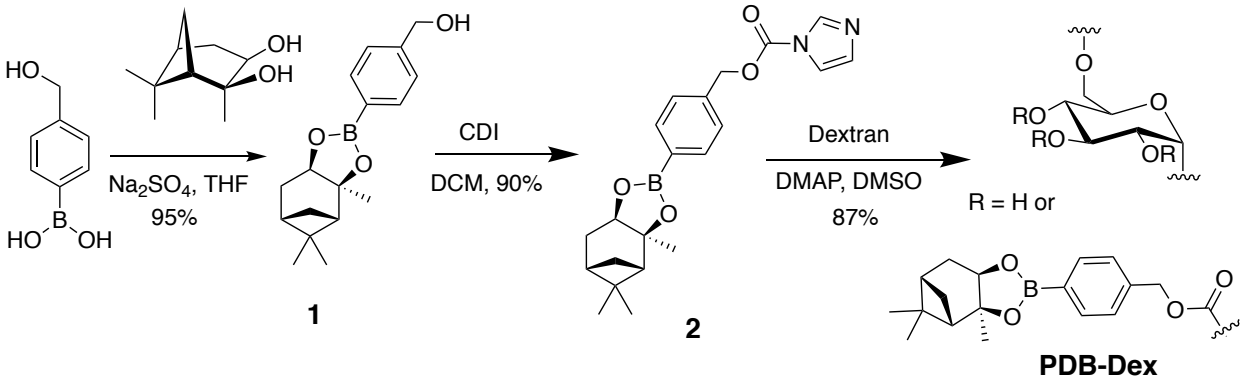

Scheme 2. Synthesis of PDB-Dex. Hydroxymethylphenyl boronic is converted to PDB ester **1**, then activated with CDI forming imidazole carbamate **2**. DMAP-catalyzed grafting to dextran to yields PDB-Dex.

To test processability, PDB-Dex polymer was converted into MPs through both nanoprecipitation and an emulsion-evaporation techniques.[21] Prior reports of PinB-Dex particles showed inconsistently sized and aggregation-prone particles, with rough shape.[15] In contrast, scanning electron microscopy revealed that PDB-Dex particles to be clearly discrete smooth spheres with an average diameter of 325 ± 150 nm (Figure 2a and S2). Dynamic light scattering measurements confirmed a size of 331 ± 173 nm and that MPs can be completely redispersed from the solid state (Figure S2). This diameter is within the desired range for passive targeting of APCs.[6] For other applications, the size of nanoparticles can be tuned in a similar fashion to processing of other hydrophobic polymers like PLGA. To demonstrate this, nanoprecipitation particles were prepared with sizes ranging from 203 ± 78 nm down to 40 ± 7 nm (Figure S3).

Although the poor solubility of PinB-Dex prevents preparation of MP through most standard means, partial dissolution followed by filtering allows for the preparation of small amounts of PinB-Dex MPs by nanoprecipitation. This allowed for the comparison of zeta potential of PinB-Dex and PDB-Dex MP. Interestingly, the zeta potential was not identical between these samples, and were −45 ± 1 and −23 ± 2 mV respectively. We can attribute this difference to a decreased fraction of boron in the tetrahedral anionic state in PDB-Dex due to increased steric bulk around the boron center.[26]

Although PDB-Dex has better material properties than PinB-Dex, we wondered whether the changes made to the boronic ester affected the mechanism of degradation. To evaluate this, particles were suspended in buffered deuterated water containing deuterium peroxide and the

release of soluble degradation products was measured *in situ* by NMR (Figure 2b and S4). As expected, dextran, PD, and hydroxybenzyl alcohol (HBA) were all released into solution as PDB-Dex particles degraded and dissolved. The appearance of each component was fit empirically and the ratio of final concentrations after 20 h matched prior characterization. Somewhat unexpectedly, the oxidation-triggered cleavage occurred in three discrete steps. PD is released into solution at twice the rate of HBA, indicating that C–B oxidation occurs significantly more quickly than 1,4-elimination. The appearance of dextran in solution only occurs after a sufficient proportion of modifications have completely eliminated from the polymer backbone.

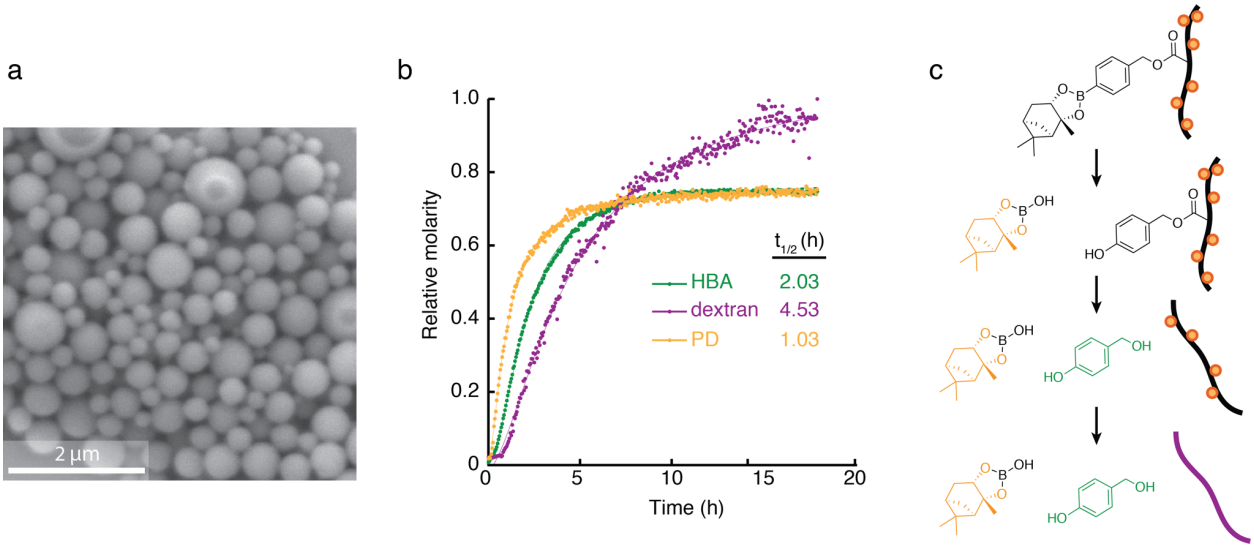

Figure 2. Preparation and degradation of PDB-Dex emulsion MPs. (**a**) Spherical morphology of emulsion MPs by SEM is indicative of good processability. **(b**) PDB-Dex incubated with aqueous deuterium peroxide and monitored by NMR to observe the appearance of the degraded components of the modified polymer: dextran (magenta), 4-hydroxybenzyl alcohol (green), and PD (orange). **(c)** Stepwise degradation of PDB-Dex consistent with NMR data.

While the NMR spectroscopy gave a clear representation of the mechanism of degradation, a relatively high concentration of MPs is required to produce sufficient signal strength. Because

oxidation-triggered degradation requires stoichiometric equivalents of peroxide, the concentration of peroxide in this experiment is too high to appropriately represent that of a cellular environment. To better mimic biological conditions, we degraded MPs under biologically relevant concentrations of hydrogen peroxide, and measured the release of dextran into solution using an adapted bicinchoninic acid (BCA) copper reduction assay (Figure 3). Although oxidizing agents like hydrogen peroxide can interfere with redox-mediated assays, we were able to overcome this through catalytic decomposition of hydrogen peroxide with potassium iodide. PDB-Dex was observed to degrade in a dose-dependent manner: degradation was observed to be significantly faster than background hydrolysis in the presence of 1 mM and 0.1 mM H_2O_2. At 0.01 mM H_2O_2, degradation does not appear to be significantly faster than background.

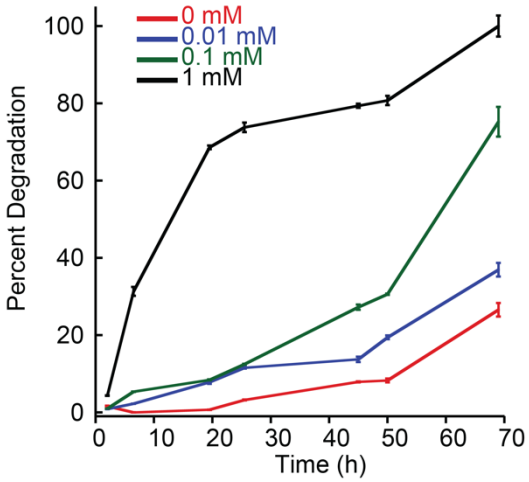

Figure 3. Concentration-dependent PDB-Dex Degradation of PDB-Dex emulsion MPs by H_2O_2 expressed via BCA Assay. Aliquots taken from degrading microparticle suspensions were centrifuged to remove intact MPs, then soluble polysaccharide was quantified colorimetrically using a BCA assay.

To further demonstrate the processability of PDB-Dex and investigate its potential in a vaccine formulation, a monoaxial electrospray (ES) method was used to generate PDB-Dex MPs. As

opposed to other commonly-employed methods of MP manufacture such as emulsion/solvent evaporation,[29] ES is a continuous, scalable manufacturing process that enables high encapsulation efficiency of compounds with diverse physicochemical properties.[30–32] In addition, ES does not expose cargos to the high shear forces generally required for the generation of emulsions, which can degrade or denature sensitive protein antigens and subsequently reduce their antigenicity.[33,34] Using a laboratory-scale monoaxial ES setup as previously described,[24] we fabricated PDB-Dex MPs loaded with the imidazoquinoline resiquimod, a potent hydrophobic adjuvant targeting toll-like receptor (TLR) 7/8 expressed in the endosomes in APCs.[35] The resultant MPs were approximately 1 μm in diameter (Figure 4). This size is within the range expected for this technique, and is appropriate for applications in immunotherapy. Additionally, prior work has shown that ES MPs can be taken up by APCs and are trafficked to the lymph node.[33] Although larger spherical MPs would be expected to have slightly reduced rates of degradation based on a decrease in surface-area-to-volume ratio,[36] ES MPs possess wrinkled morphologies that lead to greater surface area than a sphere of corresponding diameter.

The encapsulation of resiquimod was confirmed dissolving MPs in DMSO and performing fluorescence measurements. Encapsulation efficiency was determined to be 59% (Table 1). Release of resiquimod from MPs was measured in the presence of absence of 0.1 mM H_2O_2 (Figure S5). After an initial period of rapid release, MPs display relatively slow release of resiquimod in PBS. In contrast, MPs demonstrate more rapid and sustained release in the presence of 0.1 mM H_2O_2.

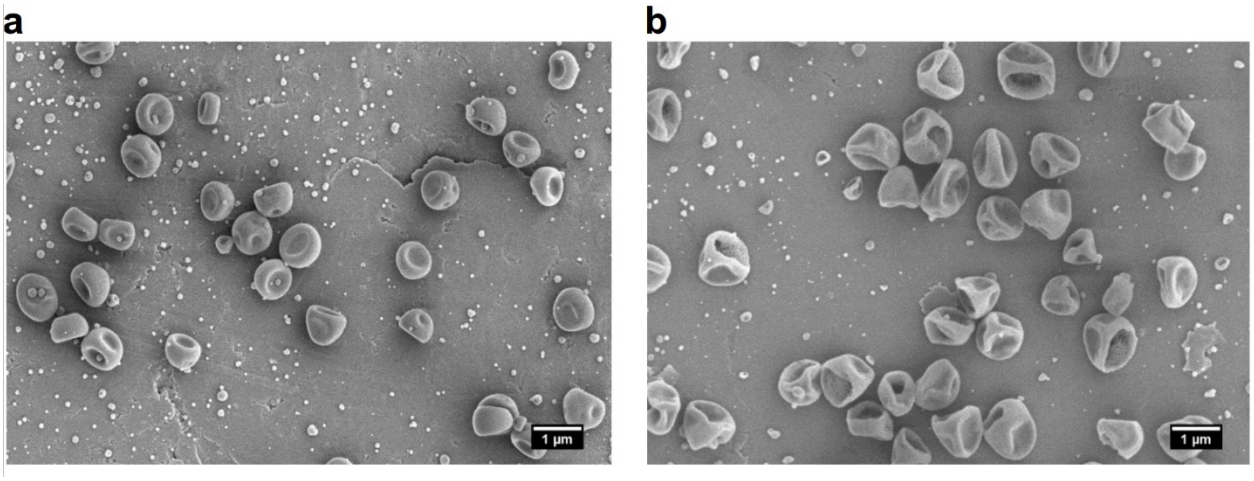

Figure 4. Representative SEM images of (**a**) blank and (**b**) resiquimod-loaded PDB-Dex electrosprayed microparticles.

Table 1. Diameter, loading, and encapsulation efficiency of electrosprayed MPs.

ES PDB-DEX Particle	*Diameter (µm)*	*Theoretical Loading (µg resi./mg MP)*	*Actual Loading (µg resi./mg MP)*	*Encapsulation Efficiency (%)*
Blank	0.81 ± 0.06	-----	-----	-----
Resiquimod	1.00 ± 0.11	10	5.9	59%

We examined the effects of ES PDB-Dex microparticles on cell viability and proinflammatory cytokine secretion in vitro by treating murine bone marrow derived dendritic cells (BMDCs) with unloaded and resiquimod loaded PDB-Dex MPs for 24 and 72 hours. BMDC viability tied with proliferation was evaluated using a 3-(4,5-dimethylthiazol-2-yl)-2,5-diphenyltetrazolium bromide (MTT) assay (Figure 5), while secretion of proinflammatory cytokines IL-6 and TNF-α was quantified using an enzyme-linked immunosorbent assay (ELISA) (Figure 6). There was no significant reduction in cell viability due to PDB-Dex MPs after 72 hours at any dose evaluated. MP-formulated resiquimod elicited similar, but slightly lower, secretion of both IL-6 and TNF-α

at all doses tested compared to soluble resiquimod. This could potentially be related to the controlled release of the MPs that initially would be mediated through diffusion and then accelerated oxidation-dependent degradation. The effects of this controlled release system can be observed by the level of secreted IL-6, which increased slightly from 24 to 72 hours after resiquimod-loaded MP treatment, while it decreased in the same time frame after free drug treatment. This extended therapeutic window is indicative of controlled longer-term release of cargo.

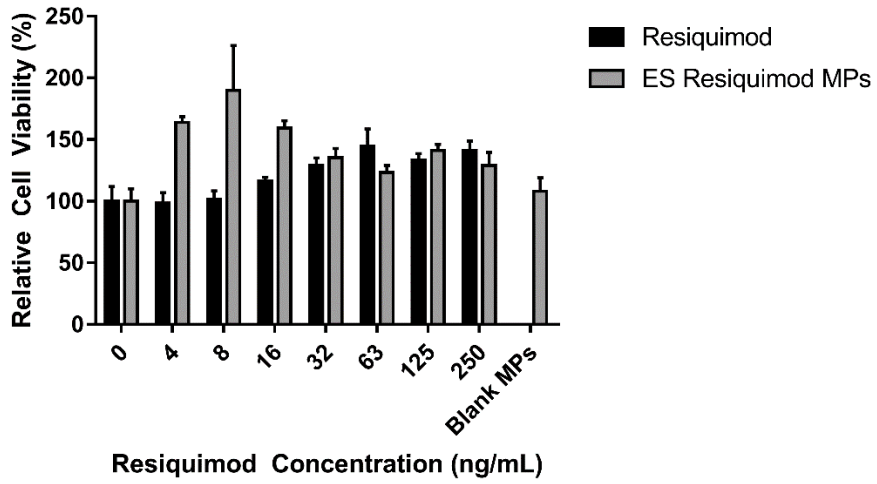

Figure 5: BMDCs were treated with blank PDB-Dex MPs or a range of concentrations of free resiquimod or resiquimod-loaded PDB-Dex MPs for 72 hours, and an MTT assay was used to determine cell viability. Viability remained high across all treatment groups.

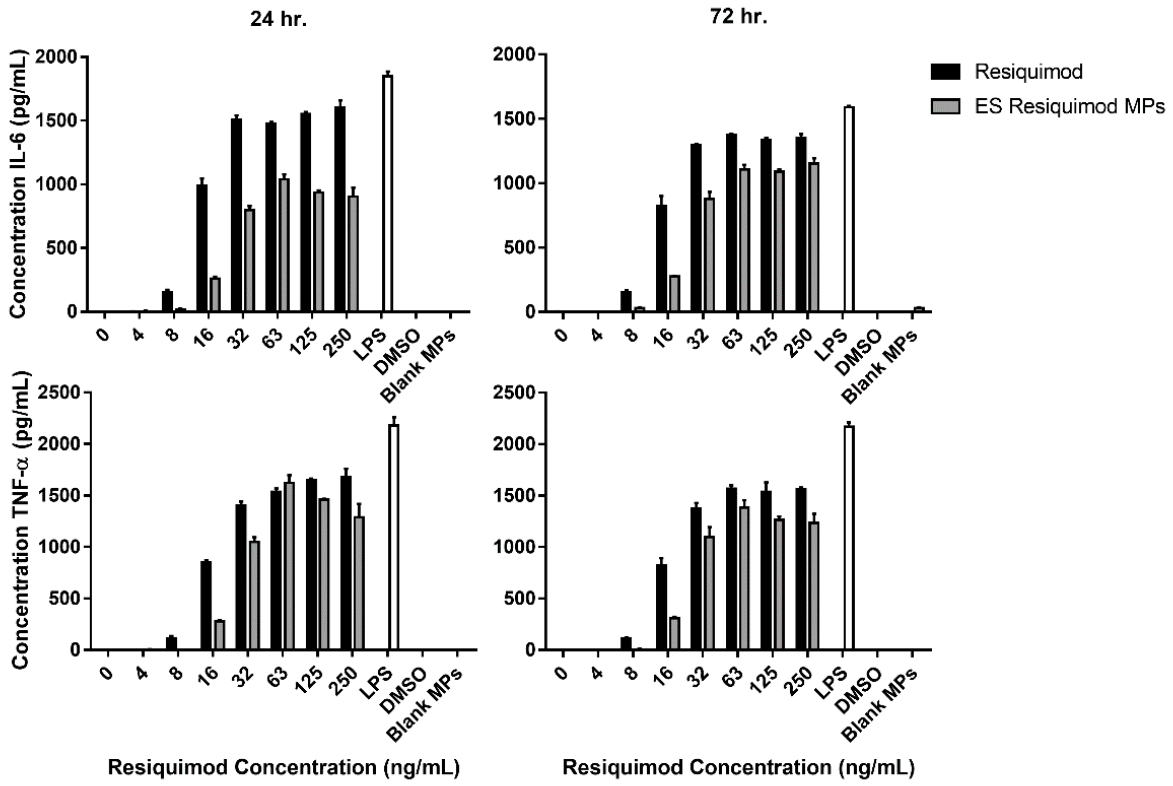

Figure 6: BMDCs were treated with blank PDB-Dex MPs or a range of concentrations of free resiquimod or resiquimod-loaded PDB-Dex MPs for 24 and 72 hours, and their secretion of proinflammatory cytokines IL-6 and TNF-α was quantified by ELISA.

Conclusions

Here we report the generation of an oxidation-sensitive modified dextran, for application in the high oxidative stress environment of the APC phagosome. Pin-modified aryl boronic esters are widely used in molecular sensors and oxidation sensitive vehicles. Early efforts to capitalize on this group for solubility switching of modified dextrans have shown promise, but continued work is hampered by poor solubility and inconsistent processability. We hypothesized that this deficit is caused by the transesterification of the added Pin boronic esters to yield dextran boronic esters,

which crosslink the polymer chains. We thus investigated alternative diols and found that aryl boronic esters made with PD are stable to transesterification with the diols present on dextran.

We have synthesized PDB-Dex as an aryl-boronate modified dextran polymer, and find that it has favorable solubility and processing properties upon repeated concentration and redissolution. Additionally, PDB-Dex retains the expected oxidative sensitivity of other aryl boronic esters. In the presence of hydrogen peroxide PDB-Dex degrades into dextran, 4-hydroxybenzyl alcohol and PD borate. Interestingly, the triggered degradation of PDB-Dex microparticles appears to occur in a stepwise sequence where an appreciable concentration of phenol groups remains on the polymer before undergoing self-immolative cleavage.

To demonstrate its improved processability, we demonstrate that MPs can be formulated using emulsion, nanoprecipitation, or electrospray techniques, and find that these MPs possess H_2O_2 concentration-dependent degradation. We demonstrate the ability to encapsulate cargo by loading the TLR 7/8 agonist resiquimod in electrosprayed MPs. They induce minimal cytotoxicity, but are able to induce production of IL-6 and TNF-α in mouse BMDCs. Thus, this newly developed oxidation sensitive polymer has promise for application as a particulate immunotherapy.

ASSOCIATED CONTENT

Supporting Information.

The following files are available free of charge. Quantification of dextran branching, emulsion MP size characterization, and NMR and IR of synthesized compounds. (PDF)

AUTHOR INFORMATION

Corresponding Author

*E-mail: broaders@mtholyoke.edu

ORCID

Amanda Manaster: 0000-0002-9188-1784

Cole Batty: 0000-0002-5631-2623

Eric Bachelder: 0000-0002-8572-888X

Kristy Ainslie: 0000-0002-1820-8382

Kyle Broaders: 0000-0002-6827-8717

Notes

The authors declare no competing financial interest.

ACKNOWLEDGMENT

Work by AJM, and KEB supported by the National Science Foundation under Grant No. DMR 1808073. AJM, AO, and KEB also gratefully acknowledge the Mount Holyoke College Fund the Future Research Award for additional financial support, and Blanca Carbajal Gonzalez and Sarah Kiemle at the Mount Holyoke College Science Center Microscopy Facility for help with SEM acquisition. Research by PT was supported by the National Cancer Institute of the National Institutes of Health under award number T32CA196589.

This work was performed in part at the Chapel Hill Analytical and Nanofabrication Laboratory, CHANL, a member of the North Carolina Research Triangle Nanotechnology Network, RTNN, which is supported by the National Science Foundation, Grant ECCS-1542015, as part of the National Nanotechnology Coordinated Infrastructure, NNCI.

References

(1) Gomes, A.; Mohsen, M.; Bachmann, M. Harnessing Nanoparticles for Immunomodulation and Vaccines. *Vaccines* **2017**, *5* (1), 6. https://doi.org/10.3390/vaccines5010006.

(2) Serda, R. Particle Platforms for Cancer Immunotherapy. *International Journal of Nanomedicine* **2013**, 1683. https://doi.org/10.2147/IJN.S31756.

(3) Vartak, A.; Sucheck, S. Recent Advances in Subunit Vaccine Carriers. *Vaccines* **2016**, *4* (2), 12. https://doi.org/10.3390/vaccines4020012.

(4) Zauner, W.; Farrow, N. A.; Haines, A. M. R. In Vitro Uptake of Polystyrene Microspheres: Effect of Particle Size, Cell Line and Cell Density. *Journal of Controlled Release* **2001**, *71* (1), 39–51. https://doi.org/10.1016/S0168-3659(00)00358-8.

(5) Prabha, S.; Arya, G.; Chandra, R.; Ahmed, B.; Nimesh, S. Effect of Size on Biological Properties of Nanoparticles Employed in Gene Delivery. *Artificial Cells, Nanomedicine, and Biotechnology* **2016**, *44* (1), 83–91. https://doi.org/10.3109/21691401.2014.913054.

(6) Foged, C.; Brodin, B.; Frokjaer, S.; Sundblad, A. Particle Size and Surface Charge Affect Particle Uptake by Human Dendritic Cells in an in Vitro Model. *International Journal of Pharmaceutics* **2005**, *298* (2), 315–322. https://doi.org/10.1016/j.ijpharm.2005.03.035.

(7) Gammon, J. M.; Dold, N. M.; Jewell, C. M. Improving the Clinical Impact of Biomaterials in Cancer Immunotherapy. *Oncotarget* **2016**, *7* (13). https://doi.org/10.18632/oncotarget.7304.

(8) Sies, H. Oxidative Stress: A Concept in Redox Biology and Medicine. *Redox Biology* **2015**, *4*, 180–183. https://doi.org/10.1016/j.redox.2015.01.002.

(9) Saravanakumar, G.; Kim, J.; Kim, W. J. Reactive-Oxygen-Species-Responsive Drug Delivery Systems: Promises and Challenges. *Advanced Science* **2017**, *4* (1), 1600124. https://doi.org/10.1002/advs.201600124.

(10) Rehor, A.; Hubbell, J. A.; Tirelli, N. Oxidation-Sensitive Polymeric Nanoparticles. *Langmuir* **2005**, *21* (1), 411–417. https://doi.org/10.1021/la0478043.

(11) Liu, J.; Pang, Y.; Zhu, Z.; Wang, D.; Li, C.; Huang, W.; Zhu, X.; Yan, D. Therapeutic Nanocarriers with Hydrogen Peroxide-Triggered Drug Release for Cancer Treatment. *Biomacromolecules* **2013**, *14* (5), 1627–1636. https://doi.org/10.1021/bm4002574.

(12) Wu, E. C.; Park, J.-H.; Park, J.; Segal, E.; Cunin, F.; Sailor, M. J. Oxidation-Triggered Release of Fluorescent Molecules or Drugs from Mesoporous Si Microparticles. *ACS Nano* **2008**, *2* (11), 2401–2409. https://doi.org/10.1021/nn800592q.

(13) Brooks, W. L. A.; Sumerlin, B. S. Synthesis and Applications of Boronic Acid-Containing Polymers: From Materials to Medicine. *Chemical Reviews* **2016**, *116* (3), 1375–1397. https://doi.org/10.1021/acs.chemrev.5b00300.

(14) Tapeinos, C.; Pandit, A. Physical, Chemical, and Biological Structures Based on ROS-Sensitive Moieties That Are Able to Respond to Oxidative Microenvironments. *Advanced Materials* **2016**, *28* (27), 5553–5585. https://doi.org/10.1002/adma.201505376.

(15) Broaders, K. E.; Grandhe, S.; Fréchet, J. M. J. A Biocompatible Oxidation-Triggered Carrier Polymer with Potential in Therapeutics. *Journal of the American Chemical Society* **2011**, *133* (4), 756–758. https://doi.org/10.1021/ja110468v.

(16) Irving, G. W. *EVALUATION OF THE HEALTH ASPECTS OF DEXTRANS AS FOOD INGREDIENTS*; SCOGS report PB254537; Select Committee on GRAS Substances: Washington, DC, 1975.

(17) Roy, C. D.; Brown, H. C. Stability of Boronic Esters – Structural Effects on the Relative Rates of Transesterification of 2-(Phenyl)-1,3,2-Dioxaborolane. *Journal of Organometallic Chemistry* **2007**, *692* (4), 784–790. https://doi.org/10.1016/j.jorganchem.2006.10.013.
(18) Akgun, B.; Hall, D. G. Fast and Tight Boronate Formation for Click Bioorthogonal Conjugation. *Angewandte Chemie International Edition 55* (12), 3909–3913. https://doi.org/10.1002/anie.201510321.
(19) Clary, J. W.; Rettenmaier, T. J.; Snelling, R.; Bryks, W.; Banwell, J.; Wipke, W. T.; Singaram, B. Hydride as a Leaving Group in the Reaction of Pinacolborane with Halides under Ambient Grignard and Barbier Conditions. One-Pot Synthesis of Alkyl, Aryl, Heteroaryl, Vinyl, and Allyl Pinacolboronic Esters. *The Journal of Organic Chemistry* **2011**, *76* (23), 9602–9610. https://doi.org/10.1021/jo201093u.
(20) Morandi, F.; Caselli, E.; Morandi, S.; Focia, P. J.; Blázquez, J.; Shoichet, B. K.; Prati, F. Nanomolar Inhibitors of AmpC β-Lactamase. *Journal of the American Chemical Society* **2003**, *125* (3), 685–695. https://doi.org/10.1021/ja0288338.
(21) Beaudette, T. T.; Cohen, J. A.; Bachelder, E. M.; Broaders, K. E.; Cohen, J. L.; Engleman, E. G.; Fréchet, J. M. J. Chemoselective Ligation in the Functionalization of Polysaccharide-Based Particles. *J. Am. Chem. Soc.* **2009**, *131* (30), 10360–10361. https://doi.org/10.1021/ja903984s.
(22) Liebert, T.; Hornig, S.; Hesse, S.; Heinze, T. Nanoparticles on the Basis of Highly Functionalized Dextrans. *Journal of the American Chemical Society* **2005**, *127* (30), 10484–10485. https://doi.org/10.1021/ja052594h.
(23) Bachelder, E. M.; Beaudette, T. T.; Broaders, K. E.; Dashe, J.; Fréchet, J. M. J. Acetal-Derivatized Dextran: An Acid-Responsive Biodegradable Material for Therapeutic Applications. *Journal of the American Chemical Society* **2008**, *130* (32), 10494–10495. https://doi.org/10.1021/ja803947s.
(24) Duong, A. D.; Sharma, S.; Peine, K. J.; Gupta, G.; Satoskar, A. R.; Bachelder, E. M.; Wyslouzil, B. E.; Ainslie, K. M. Electrospray Encapsulation of Toll-Like Receptor Agonist Resiquimod in Polymer Microparticles for the Treatment of Visceral Leishmaniasis. *Molecular Pharmaceutics* **2013**, *10* (3), 1045–1055. https://doi.org/10.1021/mp3005098.
(25) Alpan, O.; Bachelder, E.; Isil, E.; Arnheiter, H.; Matzinger, P. "Educated" Dendritic Cells Act as Messengers from Memory to Naive T Helper Cells. *Nature Immunology* **2004**, *5* (6), 615–622. https://doi.org/10.1038/ni1077.
(26) Hall, D. G. Structure, Properties, and Preparation of Boronic Acid Derivatives. Overview of Their Reactions and Applications. In *Boronic Acids*; Hall, D. G., Ed.; Wiley-VCH Verlag GmbH & Co. KGaA: Weinheim, FRG, 2006; pp 1–99. https://doi.org/10.1002/3527606548.ch1.
(27) Vettori, M. H. P. B.; Franchetti, S. M. M.; Contiero, J. Structural Characterization of a New Dextran with a Low Degree of Branching Produced by Leuconostoc Mesenteroides FT045B Dextransucrase. *Carbohydrate Polymers* **2012**, *88* (4), 1440–1444. https://doi.org/10.1016/j.carbpol.2012.02.048.
(28) Roy, C. D.; Brown, H. C. A Study of Transesterification of Chiral (–)-Pinanediol Methylboronic Ester with Various Structurally Modified Diols. *Monatshefte für Chemie - Chemical Monthly* **2007**, *138* (8), 747–753. https://doi.org/10.1007/s00706-007-0681-7.
(29) Jain, R. A. The Manufacturing Techniques of Various Drug Loaded Biodegradable Poly(Lactide-Co-Glycolide) (PLGA) Devices. *Biomaterials* **2000**, *21* (23), 2475–2490. https://doi.org/10.1016/S0142-9612(00)00115-0.

(30) Bocanegra, R.; Galán, D.; Márquez, M.; Loscertales, I. G.; Barrero, A. Multiple Electrosprays Emitted from an Array of Holes. *Journal of Aerosol Science* **2005**, *36* (12), 1387–1399. https://doi.org/10.1016/j.jaerosci.2005.04.003.
(31) Chakraborty, S.; Liao, I.-C.; Adler, A.; Leong, K. W. Electrohydrodynamics: A Facile Technique to Fabricate Drug Delivery Systems. *Advanced Drug Delivery Reviews* **2009**, *61* (12), 1043–1054. https://doi.org/10.1016/j.addr.2009.07.013.
(32) Zhang, L.; Huang, J.; Si, T.; Xu, R. X. Coaxial Electrospray of Microparticles and Nanoparticles for Biomedical Applications. *Expert Review of Medical Devices* **2012**, *9* (6), 595–612. https://doi.org/10.1586/erd.12.58.
(33) Junkins, R. D.; Gallovic, M. D.; Johnson, B. M.; Collier, M. A.; Watkins-Schulz, R.; Cheng, N.; David, C. N.; McGee, C. E.; Sempowski, G. D.; Shterev, I.; et al. A Robust Microparticle Platform for a STING-Targeted Adjuvant That Enhances Both Humoral and Cellular Immunity during Vaccination. *J Control Release* **2018**, *270*, 1–13. https://doi.org/10.1016/j.jconrel.2017.11.030.
(34) Gallovic, M. D.; Schully, K. L.; Bell, M. G.; Elberson, M. A.; Palmer, J. R.; Darko, C. A.; Bachelder, E. M.; Wyslouzil, B. E.; Keane-Myers, A. M.; Ainslie, K. M. Acetalated Dextran Microparticulate Vaccine Formulated via Coaxial Electrospray Preserves Toxin Neutralization and Enhances Murine Survival Following Inhalational Bacillus Anthracis Exposure. *Adv Healthc Mater* **2016**, *5* (20), 2617–2627. https://doi.org/10.1002/adhm.201600642.
(35) Akira, S.; Uematsu, S.; Takeuchi, O. Pathogen Recognition and Innate Immunity. *Cell* **2006**, *124* (4), 783–801. https://doi.org/10.1016/j.cell.2006.02.015.
(36) Makadia, H. K.; Siegel, S. J. Poly Lactic-Co-Glycolic Acid (PLGA) as Biodegradable Controlled Drug Delivery Carrier. *Polymers* **2011**, *3* (3), 1377–1397. https://doi.org/10.3390/polym3031377.

Table of Contents Graphic